COBEM UBERLÂNDIA 2019

ABCM Associação Brasileira de Engenharia e Ciências Mecânicas

25th ABCM International Congress of Mechanical Engineering
October 20-25, 2019, Uberlândia, MG, Brazil

EVALUATION OF TRANSITIONAL TURBULENCE MODELS AVAILABLE IN OPEN SOURCE CFD CODES APPLIED TO AIRFOIL BOUNDARY LAYERS AT LOW REYNOLDS NUMBER

André Rezende Dessimoni Carvalho
Universidade Federal de Uberlândia
andrerezende@ufu.br

Pedro Paulo de Carvalho Brito
Instituto Tecnológico de Aeronáutica
pedropcb@ita.br

Abstract. *The present work aims to compare transitional turbulence closure models available in open source CFD codes when applied in low Reynolds number flows over airfoils. In order to ensure a coherent numerical comparison, a mesh convergence study is carried out. The models and codes are compared according to its proximity to the experimental pressure distributions and forces. In general, all of the codes showed good agreement, and the transitional closure models were capable of capturing features such as transitional bubbles that were not observed in the non-transitional closure models.*
Keywords: *Turbulence Closure Models, Boundary Layer Transition, Computational Fluid Dynamics*

1. INTRODUCTION

In the last decade, there was a significant growth of small companies focused on the designing of unmanned aerial vehicles (UAVs) for agricultural and surveillance applications. However, these types of aircraft operate at low Reynolds numbers compared to commercial aircraft, for which most the airfoils were designed. Some implications of these facts are aircraft with a large percentage of laminar flow, especially over the wings.

Laminar flow is a smooth condition where inside the boundary layer the flow behavior is regular, for most cases, until instabilities lead to more complex laminar motions which may become unstable and initiate turbulence, (Davidson, 2004). For aerodynamics applications, laminar flow is a desirable condition since the shear stress is much lower than if the flow were turbulent, which means less drag. However, at this state, the flow cannot afford high-pressure gradients, and separation can occur even at mild adverse pressure gradients. At some conditions, the separated flow can reattach and forms a laminar separation bubble. Such bubbles are typically observed on low Reynolds number of wings and at the leading edge of thin airfoils on gas turbines, (Jahanmiri, 2011). Therefore, predicting the place where the separation bubbles happen on wings and airfoils is a crucial factor for a good drag estimation since they usually dictate where the increase of friction drag occurs (transition) and they can also modify the pressure distribution, especially on thicker airfoils applications at low Reynolds.

With this in mind, it is necessary to study the capacity of the turbulence closure models available for RANS methodology implemented in well-known CFD open source codes to predict the aerodynamic characteristics of transitional flows with separation bubbles. Thereby the present work compares the wind tunnel experimental results from Genç and Kaynak (2009) and Karasu *et al.* (2013) for a NACA2415 airfoil at Reynolds $1 \cdot 10^5$ and $2 \cdot 10^5$, with the numerical results obtained with the software SU2 (Economon *et al.*, 2015) and OpenFOAM (The OpenFOAM Foundation, 2019) using four turbulence closure models, and one potential flow based software, Xfoil (Drela, 1989).

2. METHODOLOGY

It is studied the behaviour of turbulence models of open-source CFD codes when simulating low Reynolds flows over airfoils. The studies were carried out by means of SU2 v6.0.0, OpenFoam v1812, and XFoil v6.99 codes. The results, in terms of pressure coefficient (c_p) and skin friction coefficient (c_f) were compared to experimental data from the literature.

2.0.1 Turbulence Models

Four RANS turbulence closure models are used to perform the simulations in the present work: SA, $k-\omega$ SST, $kkL-\omega$ and SA-BC, for which the criteria accuracy and cost differ significantly from model to model.

The two non-transitional models used are the SA, Spalart and Allmaras (1992), and the $k-\omega$ SST proposed by Menter (1994). The first is a one-equation model developed for aerodynamic applications, in which a single model equation is solved for the eddy viscosity (turbulent viscosity), Pope (2000). The SA model has proved quite successful for aerodynamic application and has a low cost for a complete model; however, it is not a general one. The one-equation model is given by Equation (1).

$$\frac{\partial\tilde{\nu}}{\partial t}+u_j\frac{\partial\tilde{\nu}}{\partial x_j}=c_{b1}(1-f_{t2})\tilde{S}\tilde{\nu}-\left[c_{w1}-\frac{c_{b1}}{\kappa^2}f_{t2}\right]\left(\frac{\nu}{d}\right)^2+\frac{1}{\sigma}\left[\frac{\partial}{\partial x_j}\left((\nu+\tilde{\nu})\frac{\partial\tilde{\nu}}{\partial x_j}\right)+c_{b2}\frac{\partial\tilde{\nu}}{\partial x_i}\frac{\partial\tilde{\nu}}{\partial x_i}\right] \tag{1}$$

In the SA model, the central quantity is the eddy viscosity (ν_t), which is expressed by $\tilde{\nu}f_{v1}$. The quantity $\tilde{\nu}$ is equal to ν_t except in the viscous region, where it is associated with ν_t by the relation $X=\tilde{\nu}/\nu$. The advantage of using the transport quantity $\tilde{\nu}$ relies on its linear behavior near the wall, which is suitable for numerical solutions. This way $\tilde{\nu}$ is defined to make the eddy viscosity linear from the log-layer to the wall using the relation given by Equation (2), where c_{v1} is usually equal to 7.1.

$$f_{v1}=\frac{X^3}{X^3+c_{v1}^3} \tag{2}$$

The SA model is not capable of predicting transition location, and when used for simulation, the location where the transition takes place has to be of previous knowledge so the trip source can be activated and the flow kept laminar where desired.

The second non-transitional model, the $k-\omega$ SST, is a two-equation model and one of the most commonly used. It is mainly used for problems where the characteristics of the boundary layer need to be well resolved, such as in aerodynamic flows. The model claims to improve one of the underlying problems of two-equation models: the incapacity of accurately predict the separation in adverse gradients flows and it is capable of switching to the standard $k-\epsilon$ in the outer region and in free-stream conditions, which avoid problems of the previous formulation by Wilcox (1988). The two-equation model of the $k-\omega$ SST are obtained by a transformation of the $k-\epsilon$ into a $k-\omega$ format, however, multiplied by $(1-F_1)$, where F_1 is equal to one at the wall region and equal to zero far away from the surface (Menter, 1994). The $k-\omega$ SST formulation is expressed by Equations (3) e (4).

$$\frac{\partial(\rho k)}{\partial t}+\frac{\partial(\rho u_j k)}{\partial x_j}=P-\beta^*\rho\omega k+\frac{\partial}{\partial x_j}\left[(\mu+\sigma_k\mu_t)\frac{\partial k}{\partial x_j}\right] \tag{3}$$

$$\frac{\partial(\rho\omega)}{\partial t}+\frac{\partial(\rho u_j\omega)}{\partial x_j}=\frac{\gamma}{\nu_t}P-\beta\rho\omega^2+\frac{\partial}{\partial x_j}\left[(\mu+\sigma_\omega\mu_t)\frac{\partial k}{\partial x_j}\right]+2(1-F_1)\frac{\rho\sigma_{\omega2}}{\omega}\frac{\partial k}{\partial x_j}\frac{\partial\omega}{\partial x_j} \tag{4}$$

In Equations (3) e (4), P is the production term, and the eddy viscosity is expressed by $\mu_t=\rho a_1 k/(max(a_1\omega,\Sigma F_2))$. All the constants for the $k-\omega$ SST model can be consulted at the work of Menter (1994) or at the NASA Langley Center website (NASA Turbulence Modeling Resource, 2019).

The two transition models used in the present work are the SA-BC, Cakmakcioglu *et al.* (2017) and the $kkL-\omega$, Abdol-Hamid (2013).

The SA-BC model is based on the standard version described by Equation (1), tested in this work as one of the non-transitional models. The main difference is that the term f_{t2} is not considered. The absence of this term is responsible for delaying the transition and the trip term is usually activated, this approach is most known as the SA-NOf_{t2} and is further explained in the work of Eca *et. al* (2007). In the SA-BC model, the term f_{t2} is also unconsidered; however, the production term of the SA-NOf_{t2} is multiplied with a γ_{BC} intermittency function in order to damp turbulence production until some transition criteria is achieved (Rumsey, 2019) and the flow can finally be considered fully turbulent. The central equation for the SA-BC model is given by Equation (5).

$$\frac{\partial\tilde{\nu}}{\partial t}+u_j\frac{\partial\tilde{\nu}}{\partial x_j}=\gamma_{BC}c_{b1}\tilde{S}\tilde{\nu}-c_{w1}f_w\left(\frac{\nu}{d}\right)^2+\frac{1}{\sigma}\left[\frac{\partial}{\partial x_j}\left((\nu+\tilde{\nu})\frac{\partial\tilde{\nu}}{\partial x_j}\right)+c_{b2}\frac{\partial\tilde{\nu}}{\partial x_i}\frac{\partial\tilde{\nu}}{\partial x_i}\right] \tag{5}$$

The γ_{BC} intermittency function is defined by $\gamma_{BC}=1-exp(-\sqrt{Term_1}-\sqrt{Term_2})$ where $Term_1$ is mainly a function of the momentum thickness Reynolds number and the experimental transition onset momentum thickness Reynolds number. The term $Term_2$ is a function of the eddy viscosity, the velocity and the distance to the nearest wall. This tree parameters compose the non-dimensional viscosity term, referred to as ν_{BC}.

The last model, the $kkL-\omega$, is a three-equation one designed to predict transition. It defers from the SA-BC model because it is not based on the coupling of turbulent models with empirical transition correlations by using intermittency profiles. The $kkL-\omega$ model uses a modified version of the two-equation eddy viscosity model $k-\omega$ coupled with an additional equation for the laminar kinetic energy. The three transport equations for the turbulent kinetic energy (k_T), the laminar kinetic energy (k_L) and the ω are expressed in Equations (6) to (8).

$$\frac{Dk_T}{Dt} = P_{k_T} + R_{BP} + R_{NAT} - \omega k_T - D_T + \frac{\partial}{\partial x_j}\left[\left(\nu + \frac{\alpha_T}{\alpha_k}\right)\frac{\partial k_T}{\partial x_j}\right] \tag{6}$$

$$\frac{Dk_L}{Dt} = P_{k_L} - R_{BP} - R_{NAT} - D_L + \frac{\partial}{\partial x_j}\left[\nu\frac{\partial k_L}{\partial_{x_j}}\right] \tag{7}$$

$$\frac{D\omega}{D_t} = C_{\omega 1}\frac{\omega}{k_T}P_{k_T} + \left(\frac{C_{\omega R}}{f_W} - 1\right)\frac{\omega}{k_T}(R_{BP} + R_{NAT}) - C_{\omega 2}\omega^2 + C_{\omega 3}f_\omega\alpha_T f_W^2\frac{\sqrt{k_T}}{d^3} + \frac{\partial}{\partial x_j}\left[\nu + \frac{\alpha_T}{\sigma_\omega}\frac{\partial\omega}{\partial x_j}\right] \tag{8}$$

In Equations (6) and (7) the terms P_{k_T} and P_{k_L} represent the production of turbulent and laminar kinetic energy, in this order, and the total kinetic energy k is the sum of P_{k_T} and P_{k_L}. The fully turbulent production, destruction and the gradient transport terms are expressed in Equation (8) by the first, third and fifth terms of the right-hand side. A more detail description of the $kkL-\omega$ can be seen in the work of Walters and Cokljat (2008).

2.1 Mesh Convergence Study

To achieve mesh independence, a grid convergence study was performed according to the best practices proposed by Roache (1994). First, it was analyzed the convergence for the normal to the wall direction (here called y-direction) and then to the tangential direction (here called x-direction). Five meshes were used for each direction. Each mesh had an increase of $\sqrt{2}$ in the number of elements compared to the previous mesh. The domain dimensions are of 100 times the airfoil chord length (c) in each direction (Figure 4-a).

SU2 code with SA-BC turbulence closure model was used to perform the analyses. This model was chosen as it was expected that it would be able to catch the transitional bubble and, hence, the tangential discretization would play a significant role. As will be shown, these expectations were confirmed.

Tables 1 and 2 show for each mesh, the number of elements on the leading edge (N_{LE}), upper side (N_{UP}), lower side (N_{LW}), total number of element normal to the wall (N_Y), tangent to the wall (N_X), total number of elements (N_{TOT}), geometric growth ratio normal to the wall (R_y), the respective values of C_L and C_D, as well as their variation in relation to the base mesh (ΔC_L and ΔC_D). These data are summarized in figures 1 and 2, where the approximately linear behavior of the coefficients as the meshes are refined, is an indication of grid convergence, according to Roache (1994). Pressure coefficients obtained for each grid are shown in Figure 3.

Although Table 2 shows that C_D values were significantly changed by refining the mesh in the x-direction, Figure 3-b indicates that the pressure coefficients were not substantially improved after the base mesh. Since the present work aims to compare the behavior of the transition phenomena by means of the position and size of the bubble, it was concluded that the base mesh was enough to catch the desired details, with a feasible computational cost. Therefore this configuration, presented in Figure 4, was used to perform the following analyses.

Table 1: Mesh convergence in normal to the wall direction.

	EX COARSE-Y	COARSE-Y	BASE	FINE-Y	EX FINE-Y
N_{LE}	100	100	100	100	100
N_{UP}	50	50	50	50	50
N_{LW}	50	50	50	50	50
N_Y	57	82	115	160	223
N_{TOT}	16364	24808	38628	59532	92505
y^+	5	2	1	1	0.5
R_y	1.2	1.14	1.1	1.068	1.05
C_L	1.011	1.017	1.024	1.026	1.027
C_D	0.01598	0.01970	0.02078	0.02043	0.02053
ΔC_L	98.76%	99.32%	100.00%	100.20%	100.30%
ΔC_D	76.88%	94.81%	100.00%	98.30%	98.80%

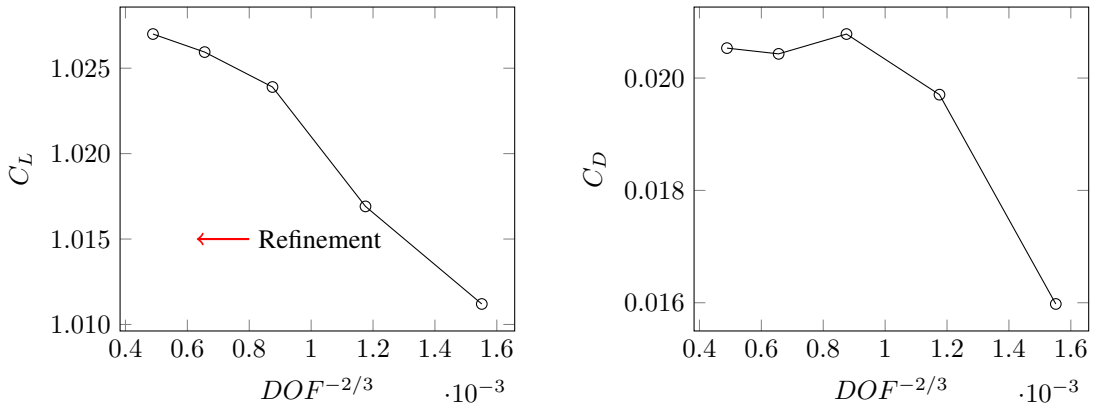

Figure 1: C_L and C_D for the normal to the wall grids plotted as function of the cells number (DOF) powered by $-2/3$.

Table 2: Mesh convergence tangent to the wall direction.

	EX COARSE-X	COARSE-X	BASE	FINE-X	EX FINE-X
N_{LE}	51	71	100	142	201
N_{UP}	26	36	50	71	101
N_{LW}	26	36	50	71	101
N_X	103	143	200	284	403
N_{TOT}	24946	30293	38628	48251	62932
R_y	1.1	1.1	1.1	1.1	1.1
y^+	1	1	1	1	1
C_L	1.034	1.037	1.024	1.007	0.992
C_D	0.02866	0.02357	0.02078	0.01795	0.01580
ΔC_L	100.85%	101.18%	100.00%	98.25%	96.81%
ΔC_D	138.16%	113.61%	100.00%	86.55%	76.18%

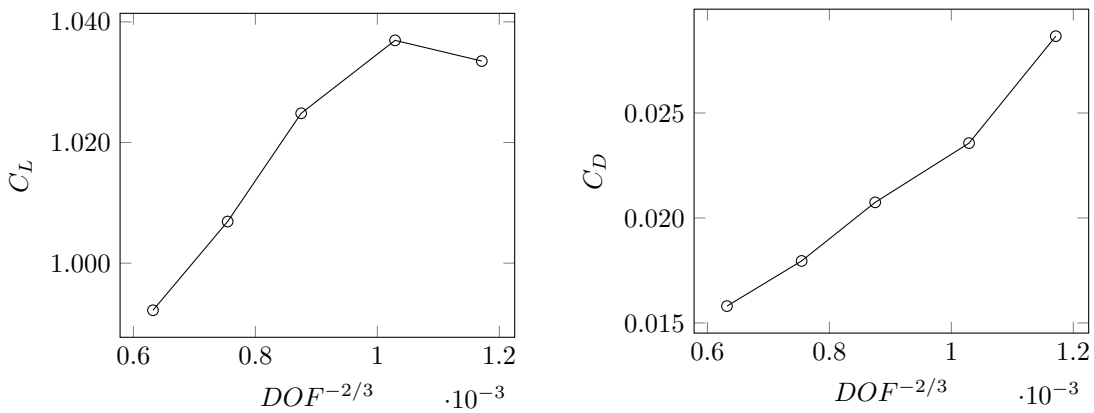

Figure 2: C_L and C_D for the tangent to the wall grids plotted as function of the cells number (DOF) powered by $-2/3$.

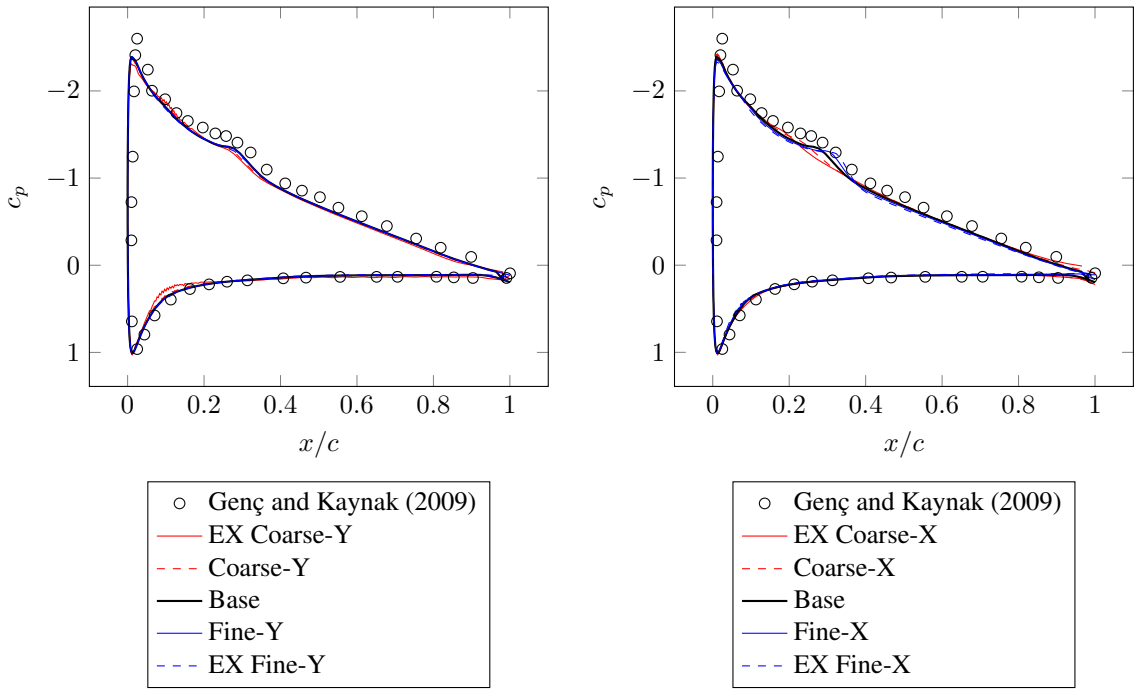

(a) y-direction. (b) x-direction.

Figure 3: Pressure coefficient for the grids analyzed in a) normal to the wall direction, and b) tangent direction.

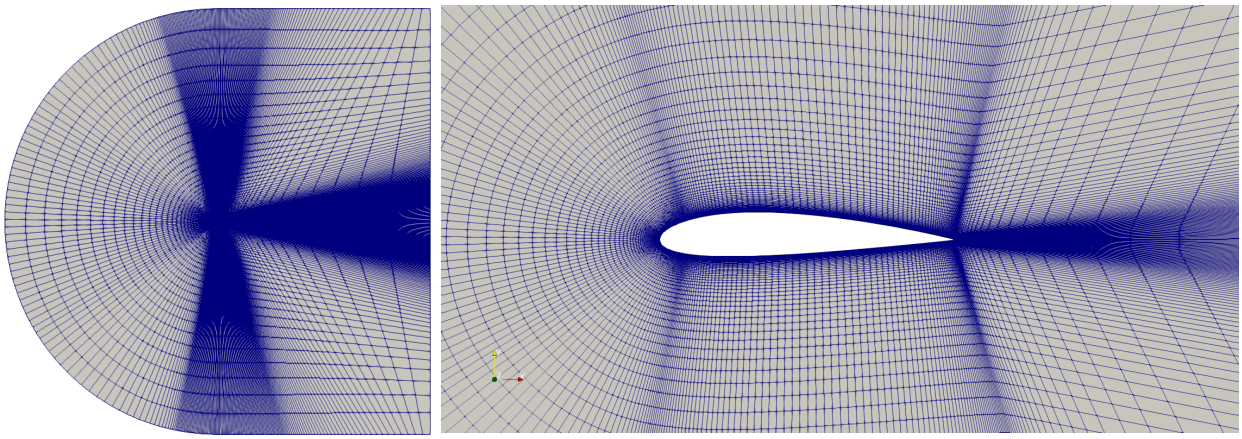

(a) Domain. (b) Airfoil

Figure 4: Base mesh.

3. RESULTS

Results obtained are shown through figures 5 and 8. Among the models presented in Figure 5, SA-BC and the KKL-ω were the only ones capable of predicting the plateau on the c_p distribution due to the transitional bubble. It is worth to note that the codes had similar behavior and results when using SST or SA for the software SU2, indicating proper implementation. Although the region of the bubble was best predicted for the KKL-ω model, for the case with $Re = 1 \cdot 10^5$, using the OpenFoam software, there was an apparent difficulty to achieve convergence, resulting in a large number of interactions and a considerable time to finish the simulation.

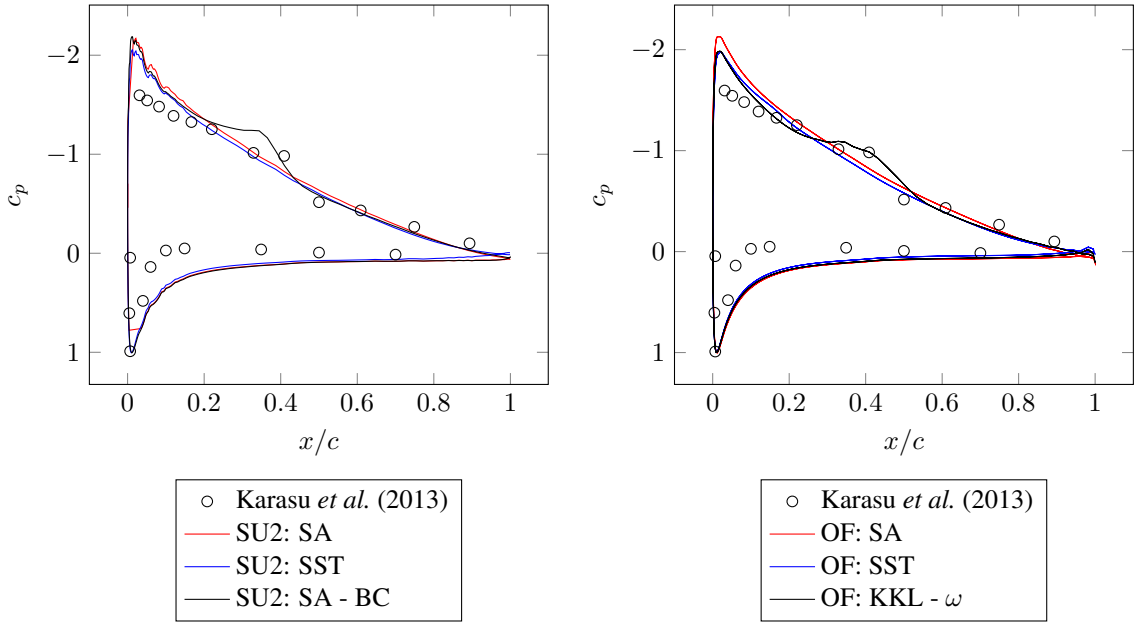

Figure 5: Pressure Coefficient for the NACA 2415 at $\alpha = 8°$ and $Re = 1 \cdot 10^5$.

Figure 6 compares the models with results from Genç and Kaynak (2009). Again, among the RANS models, SA-BC and the KKL-ω were capable of capturing the transitional bubble however, instability problems were noticed on the KKL-ω solutions. In this model, a steady solution was never achieved using the mesh shown in Figure 4 and small fluctuations in the field velocity were detected in the region where the separation bubble happens. This might be attributed to the number of mesh elements in the chord direction in the region of the bubble, not being enough to capture the physics the flow, but also indicates that for the same mesh the SA-BC model presents a more robust solution. The absence of instabilities in the SA-BC model for the present case may be due to its numerical methodology, which is coupled with intermittency functions based on experimental data, so is expected the model performs well, especially in simple geometries and 2D cases. In this case, it was added the results of the potential code XFoil, and as it can be seen, this code was the one that presented a better agreement with experimental results, despite its known simplicity, compared to RANS models.

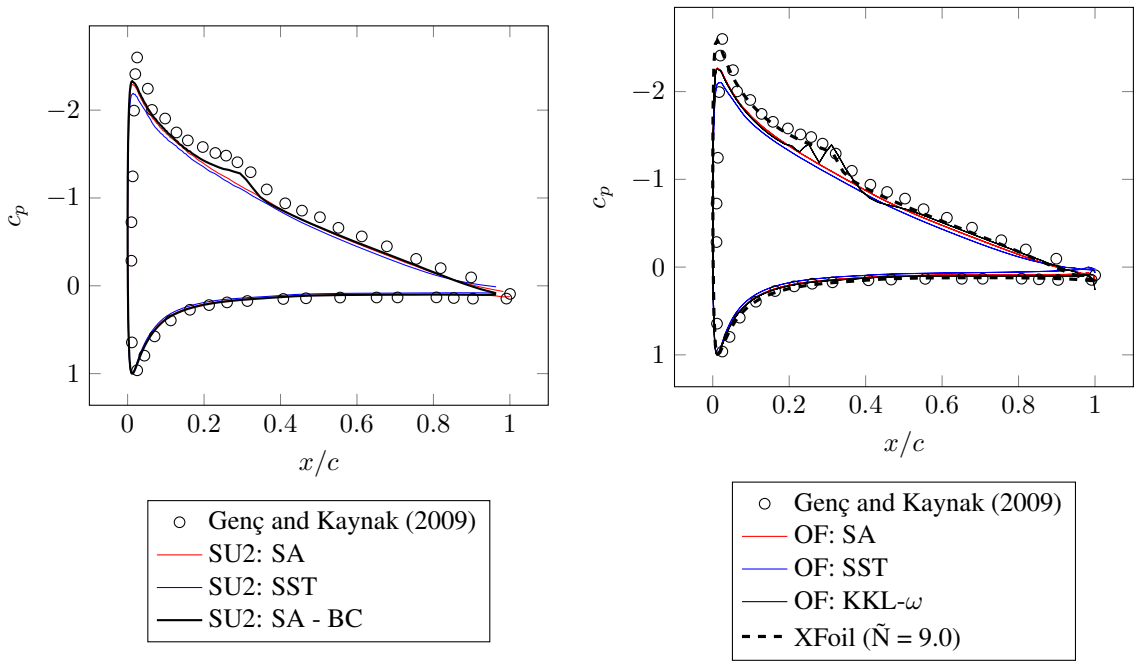

Figure 6: Pressure Coefficient solver for the NACA 2415 at $\alpha = 8°$ and $Re = 2 \cdot 10^5$.

Figure 7 shows the difference of the normalized velocity fields obtained by SA and SA-BC models from SU2 code. As it can be seen, the major difference occurs where the transitional bubble is located since, the SA model is not capable of predicting it.

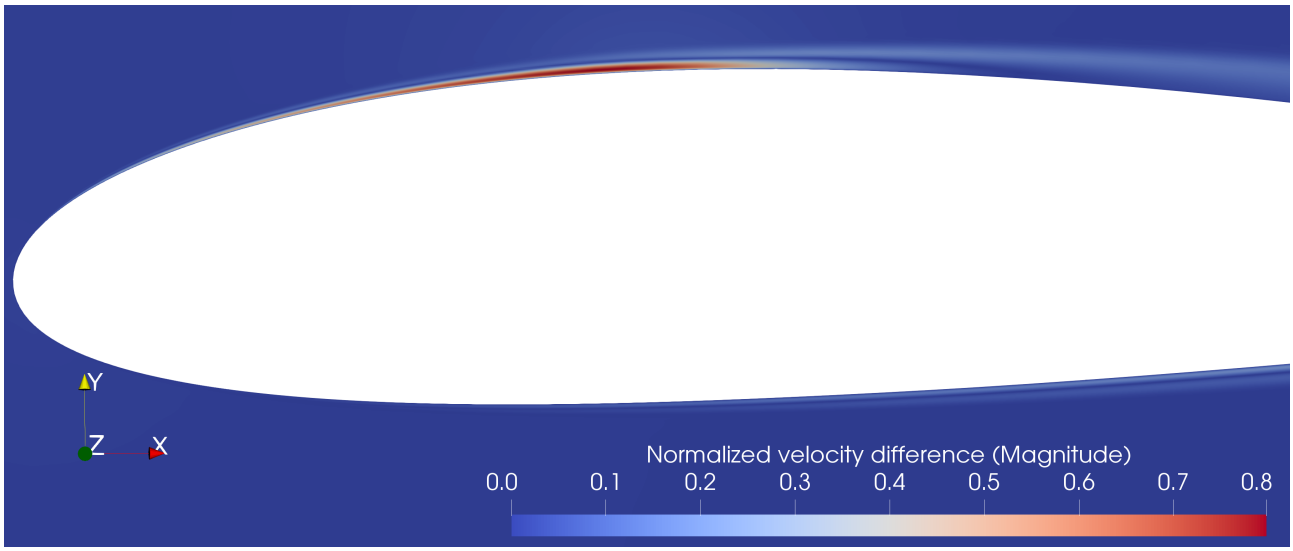

Figure 7: Difference of the normalized velocity fields obtained by SA and SA-BC models from SU2 code.

Results of skin friction coefficient (c_f) at the upper surface obtained by SU2 and OpenFoam models, XFoil and experimental results from Genç and Kaynak (2009) were compared in Figure 8. As expected, neither SA nor SST models were capable of correctly predict the laminar portion of the flow, although SST seems to start with laminar flow, but transitioning prematurely. The SA-BC, KKL-ω models and XFoil code, on the other hand, were successful at calculating both the laminar portion and the point of transition, although the KKL-ω presented some small difference at the location where the friction coefficient starts to rise.

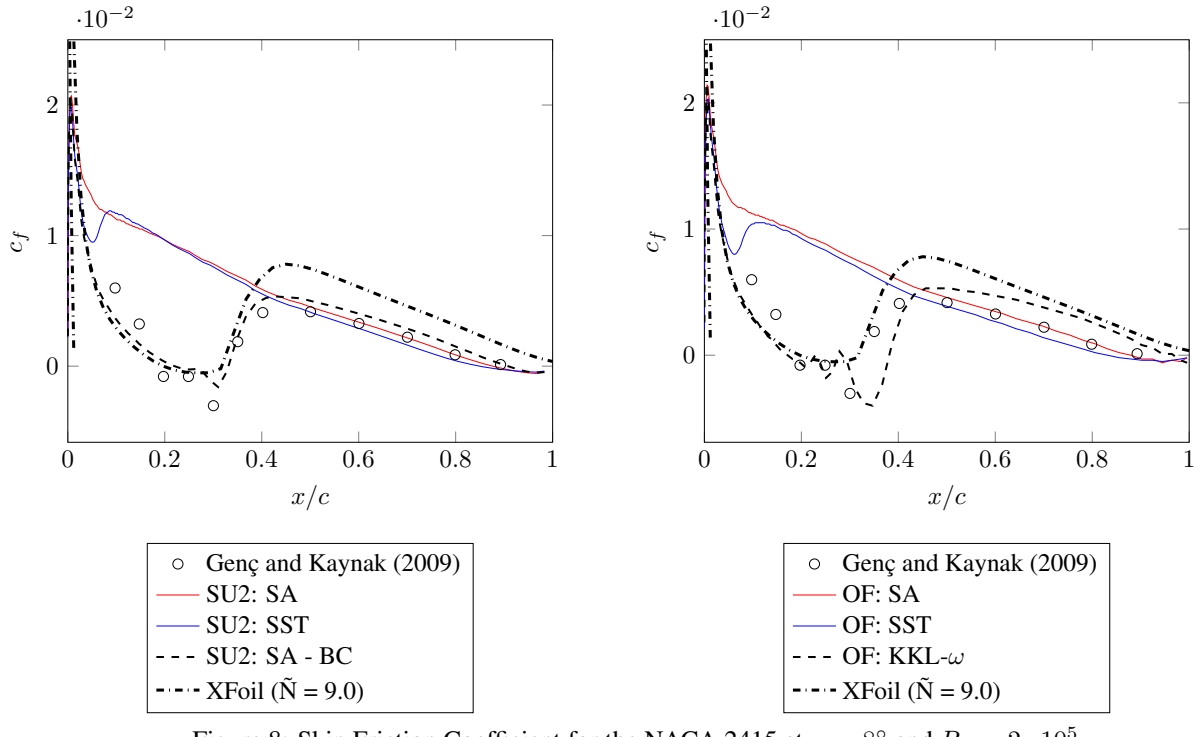

Figure 8: Skin Friction Coefficient for the NACA 2415 at $\alpha = 8°$ and $Re = 2 \cdot 10^5$.

4. CONCLUSIONS

The presented results reveal the importance of the development of robust turbulence closure models for transitional flows. It became clear that even the commonly used models, such as SST and SA, are not able to predict transition features, like transitional bubble, that have a significant impact on the aerodynamic performance of small airplanes and UAVs. Though the transitional models evaluated had shown good agreement with experimental cases, it is worth to note that they are not as numerically stable as the non-transitional, being common to face difficulties in convergence, sometimes even impossibility of convergence.

It is also worth to mention the accuracy and robustness presented by the potential code XFoil. Despite its simplicity, compared to the RANS model, it was capable of providing results as accurate as the more elaborated models, but with computational cost orders of magnitude lower, as well as significantly more straightforward pre-processing procedure.

Lastly, it is worth mention that all the models tested in the present work are calibrated with constants based on experimental results and that most of the experiments used were focused on aerospace applications (flat plates and airfoils), therefore is essential to mention that the good agreement with the type application studied in the present work sometimes may not be achieved in all type flow problems. Besides this, although the $kkL-\omega$ methodology claims to be more suitable for 3D complex geometries, where the use of models based on intermittency functions face some difficulties since most of the experimental data come from 2D tests, it is known that this model ($kkL-\omega$) uses a much higher number of constants than the other models studied in this work, which is considered a drawback and reveals the empirical nature even in the more recent RANS closure models.

5. REFERENCES

Abdol-Hamid, 2013. "Assessments of a turbulence model based on menter's modification to rotta's two-equation model". *AIAA*.

Cakmakcioglu, S.C., Bas, O. and Kaynak, U., 2017. "A correlation-based algebraic transition model". *Journal Mechanical Engineering Science*, pp. 1–15. doi:10.1177/0954406217743537.

Davidson, P.A., 2004. *Turbulence: An Introduction for Scientists and Engineers*. Oxford, New York, 1st edition.

Drela, M., 1989. "Xfoil: An analysis and design system for low reynolds number airfoils". Lecture Notes in Engineering, Springer-Verlag, New York,.

Economon, T.D., Palacios, F., Copeland, S.R., Lukaczyk, T.W. and Alonso, J.J., 2015. "Su2: An open-source suite for multiphysics simulation and design". *American Institute of Aeronautics and Astronautics*. doi:10.2514/1.J053813.

Genç, M.S. and Kaynak, U., 2009. "Control of laminar separation bubble over a naca2415 aerofoil at low re transitional flow using blowing/suction". *13th International Conference on Aerospace Sciences & Aviation Technology*.

Jahanmiri, M., 2011. "Laminar separation bubble: Its structure, dynamics ans control". <https://core.ac.uk/download/pdf/70588164.pdf>.

Karasu, I., Genç, M.S. and Açikel, H.H., 2013. "Numerical study on low reynolds number flows over an aerofoil". *Journal of Applied Mechanical Engineering*, Vol. 2, pp. 81–91.

Menter, F.R., 1994. "Two-equation eddy-viscosity turbulence models for engineering applications". *American Institute of Aeronautics and Astronautics*. doi:10.2514/3.12149.

NASA Turbulence Modeling Resource, 2019. "Nasa". URL `https://turbmodels.larc.nasa.gov/`.

Roache, P., 1994. "Perspective: A method for uniform reporting of grid refinement studies". *Journal of Fluids Engineering-transactions of The Asme - J FLUID ENG*, Vol. 116, pp. 405–413. doi:10.1115/1.2910291.

Spalart, P.R. and Allmaras, S.R., 1992. "A one-equation turbulence model for aerodynamics flows". *American Institute of Aeronautics and Astronautics*. doi:10.2514/6.1992-439.

The OpenFOAM Foundation, 2019. "Openfoam". URL `https://openfoam.org`.

Walters, D.K. and Cokljat, D., 2008. "A three-equation eddy-viscosity model for reynolds-averaged navier-stokes simulations of transitional flow". *Fluids Engineering*.

Wilcox, D.C., 1988. "Reassessment of the scale-determining equation for advanced turbulence models". *American Institute of Aeronautics and Astronautics*. doi:10.2514/3.10041.